Supplemental information for:
On the mechanism of protein-templated gold nanoparticle synthesis: Protein organization, controlled gold sequestration, and unexpected reaction products.

*Cassidy Hart, Nouf Abuladel, Madeleine Bee, Megan Channell, Alexander C. CVitan, Moira M. Esson, Andrew Farag, Trisha Ibeh, Eleni N. Kalivas, Daniel-Mario Larco, Andrew Long, Loukas Lymperopoulos, Zachary Mendel, Nancy Miles, Carly Montanero, James C. Schwabacher, Helen Slucher, Javier Vinals, John M. Heddleston[a,†], Wenyue Li, Douglas M. Fox, Matthew R. Hartings**
Department of Chemistry, American University, 4400 Massachusetts Ave, NW, Washington, DC 20016, USA
[a]Semiconductor and Dimensional Metrology Division, National Institute of Standards and Technology, Gaithersburg, MD 20899, USA
*Corresponding Author – hartings@american.edu

Contents

I. Protein-AuNP and protein-AuNP fiber reaction products.

BSA-AuNP reaction products

A full set of reaction products for BSA can be found in one of our previous publications.[1]

S1. Catalase-AuNP reaction products

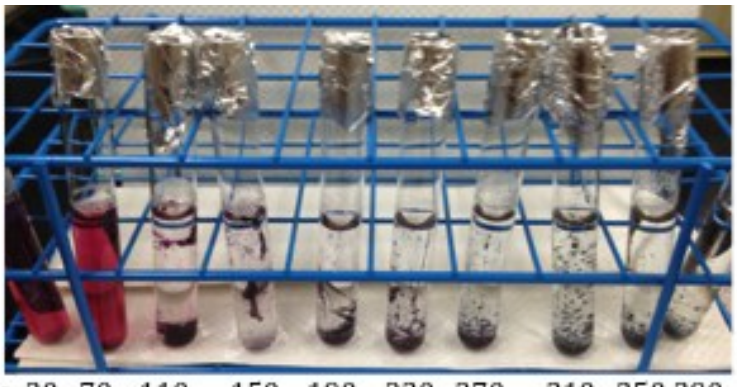

S2. Hemoglobin-AuNP reaction products

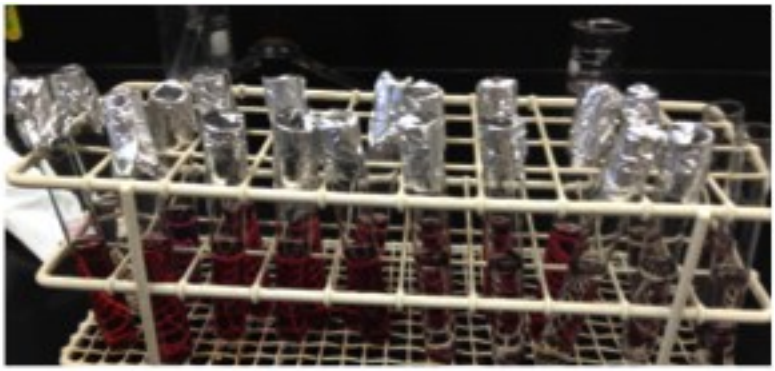

Au:Hb Ratio 7.5 13 18 23 28 33 38 43 48 53

S3. Invertase-AuNP reaction products

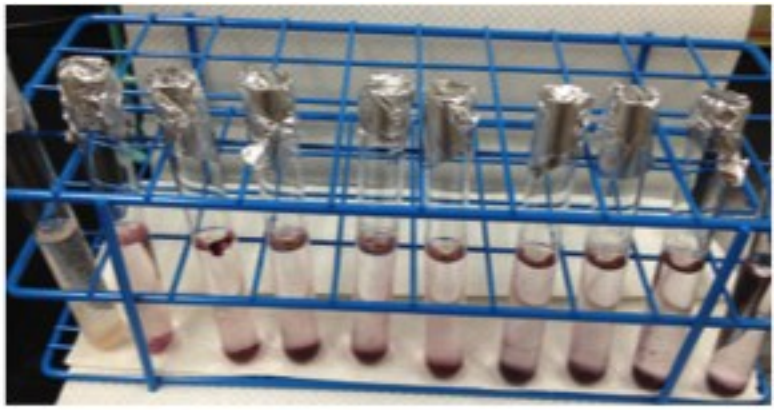

Au:Pepsin Ratio 30 70 110 150 190 230 270 310 350 390

S4. Lysozyme-AuNP reaction products

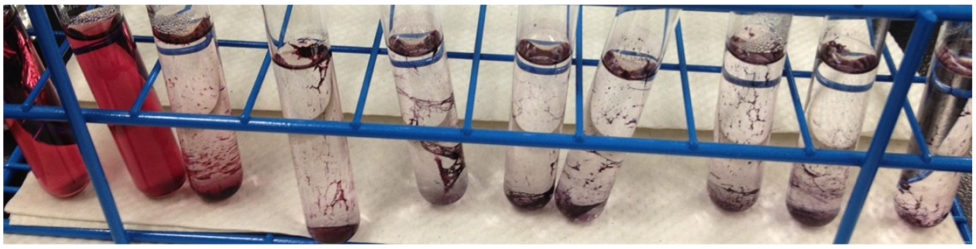

25 30 35 40 45 50 55 60 65 70
Au:Lysozyme ratio

S5. Myoglobin-AuNP reaction products

Au:Mb ratios

20 30 40 50 60 70 80 90 100 ∞

S6. Pepsin-AuNP reaction products

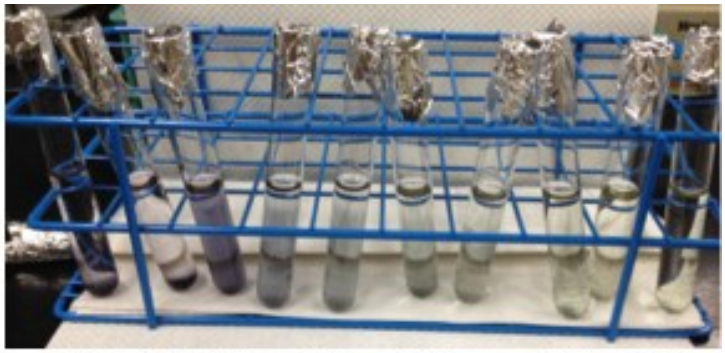

Au:Pepsin Ratio 30 70 110 150 190 230 270 310 350 390

II. TEM data

TEM images were taken using a Philips Electronic Instruments Company EM400T instrument and analyzed using the AnalySIS FIVE software program. In all images, the scale bar is 200nm.

S7. TEM image of BSA-AuNP fibers at a Au:BSA ratio of 125

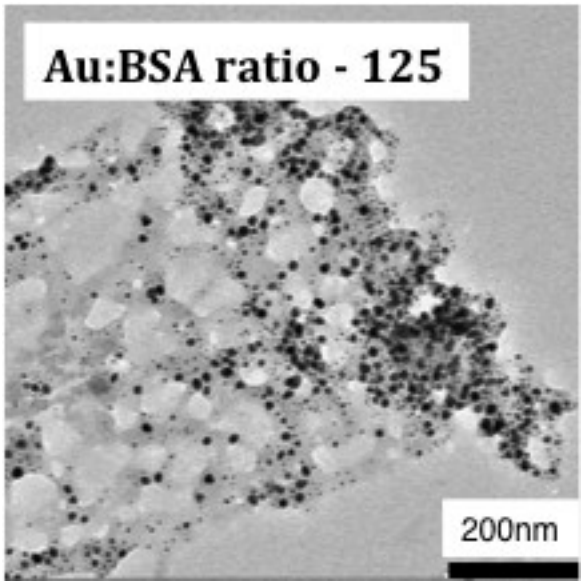

S8. TEM image of Catalase-AuNP fibers at a Au:Catalase ratio of 150

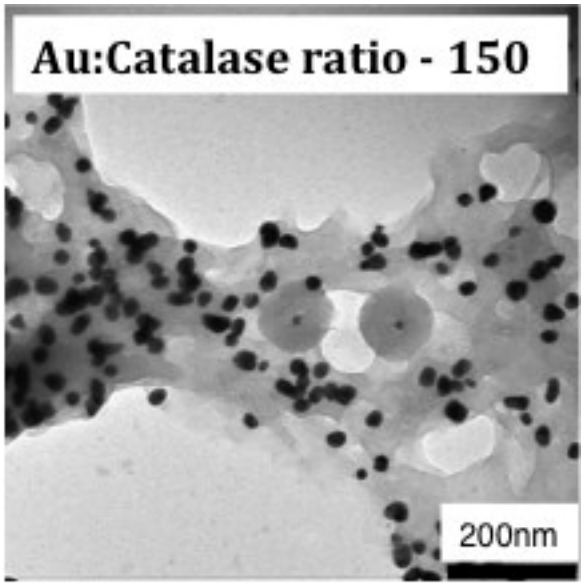

S9. TEM image of Invertase-AuNP fibers at a Au:Invertase ratio of 70

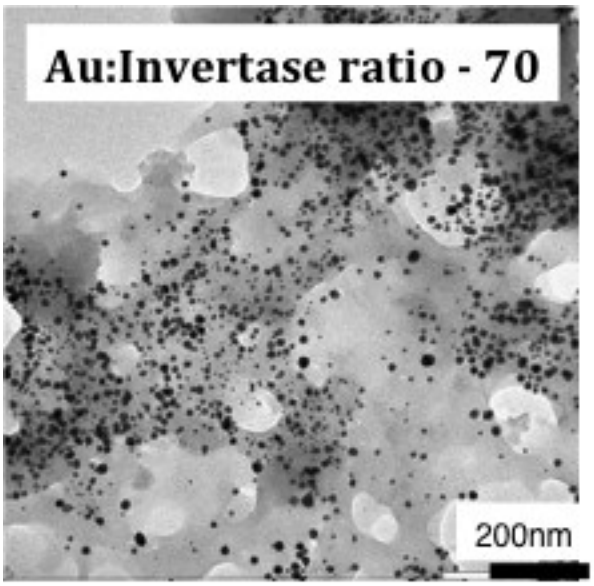

S10. TEM image of Myoglobin-AuNP fibers at a Au:Myoglobin ratio of 55

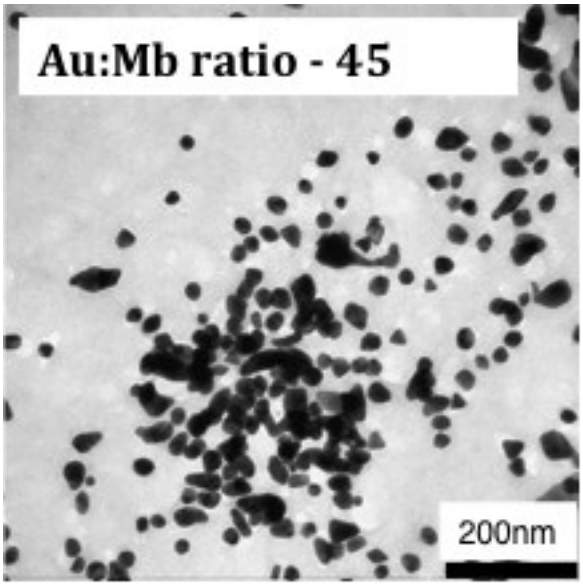

III. Particle area histograms

S11. Histogram of BSA-AuNP particle sizes at a Au:BSA ratio of 125

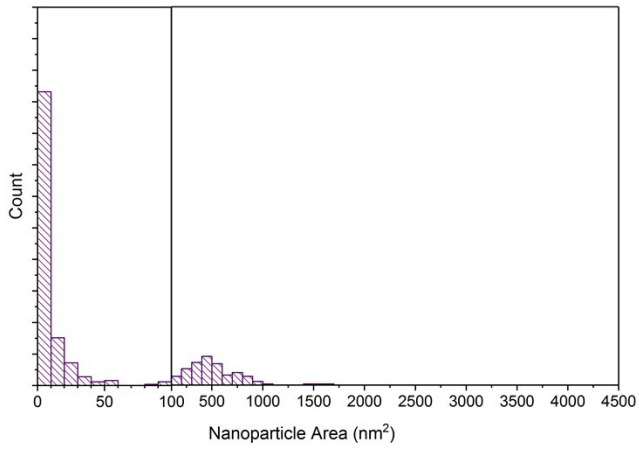

S12. Histogram of catalase-AuNP particle sizes at a Au:catalase ratio of 150

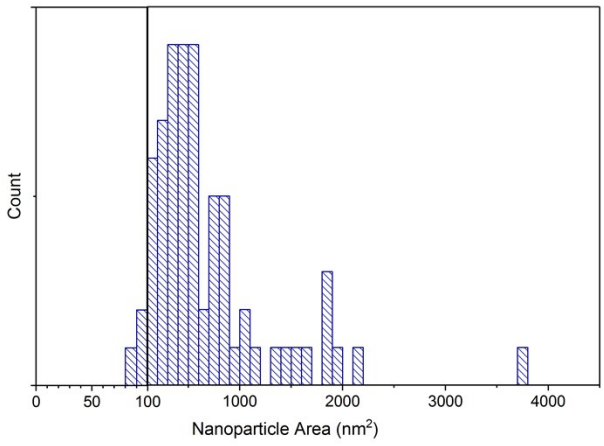

S13. Histogram of hemoglobin-AuNP particle sizes at a Au:hemoglobin ratio of 48

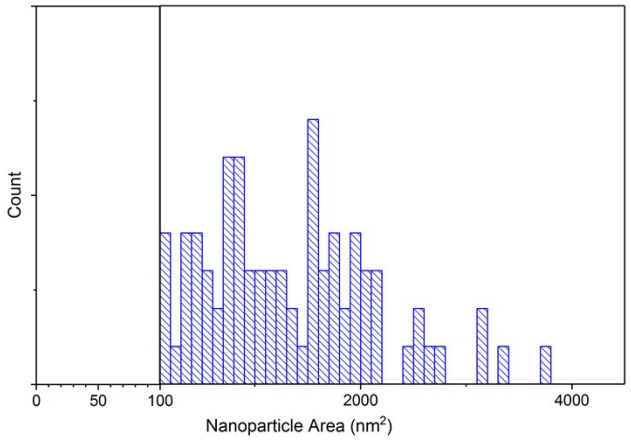

S14. Histogram of lysozyme-AuNP particle sizes at a Au:lysozyme ratio of 45

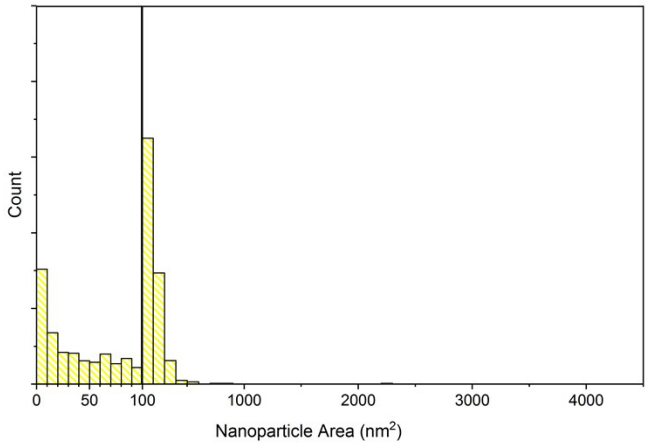

S15. Histogram of myoglobin-AuNP particle sizes at a Au:myoglobin ratio of 55

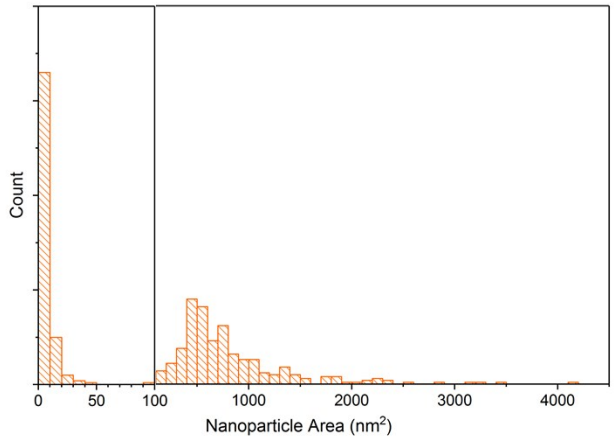

IV. UV-Vis and AA data.

There are four distinct types of Au populations that are described in the UV-Vis. 1) No observed biotemplating reaction. 2) AuNP formation. 3) Precipitated protein-Au clusters. 4) AuNP-fiber formation. Several aspects of these graphs should be noted. 1) The individual proteins do not display each population described. 2) Population #4 only occurs at very low protein concentrations. 3) Some of the traces for fiber formation show some absorbance at 530 due to some of the fibers floating in solution after the centrifugation step.

S16. UV-Vis spectra of BSA biotemplating reactions

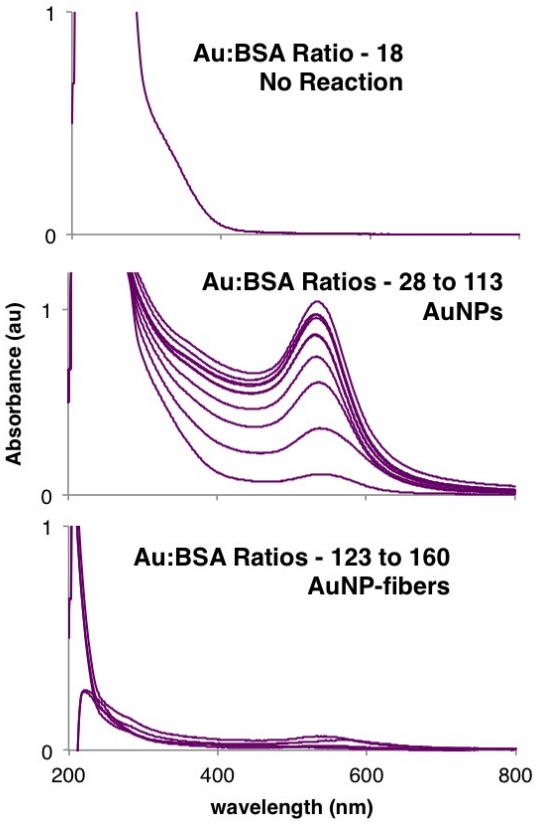

S17. UV-Vis spectra of catalase biotemplating reactions

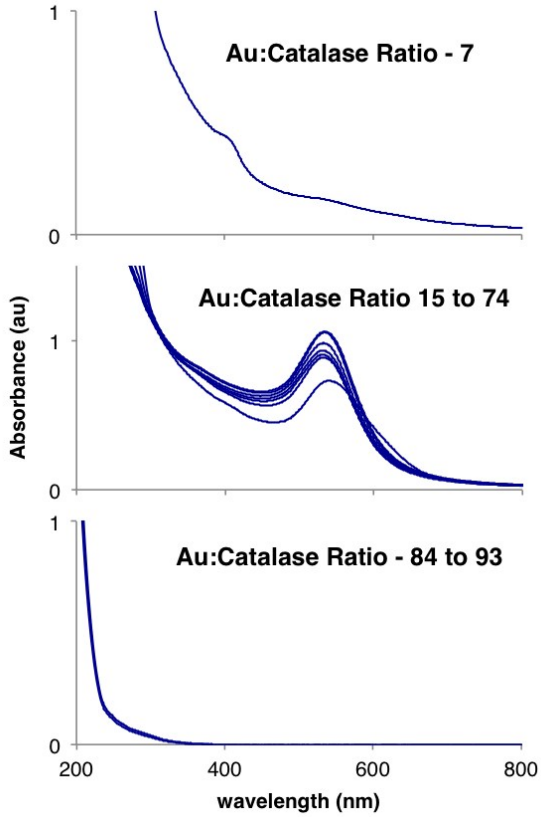

S18. UV-Vis spectra of hemoglobin biotemplating reactions

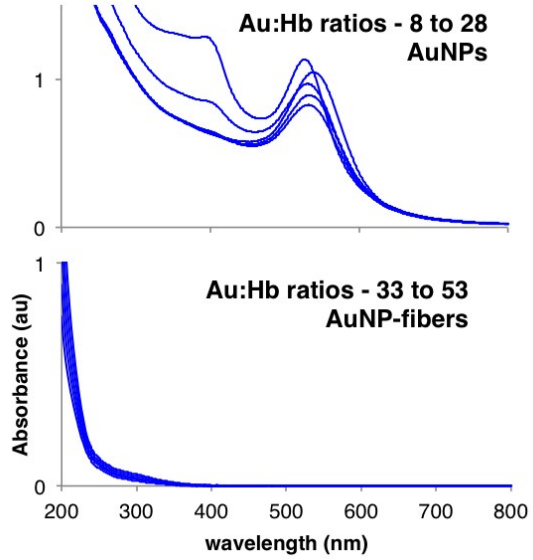

S19. UV-Vis spectra of lysozyme biotemplating reactions

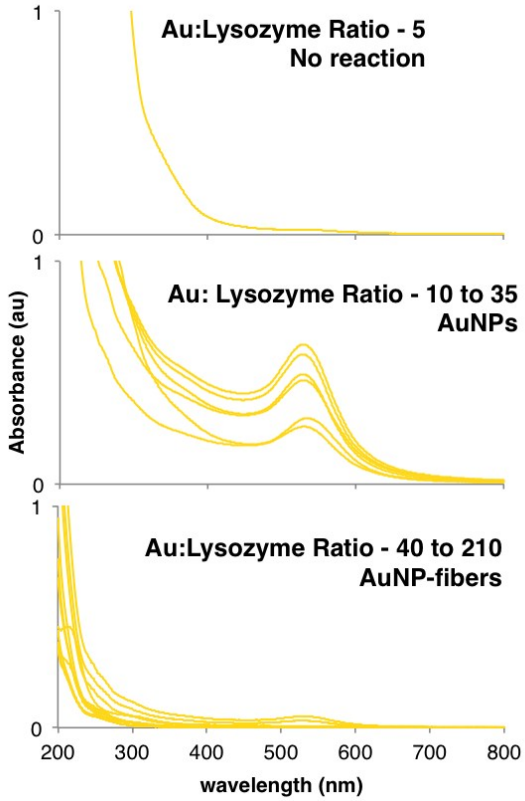

S20. UV-Vis spectra of myoglobin biotemplating reactions

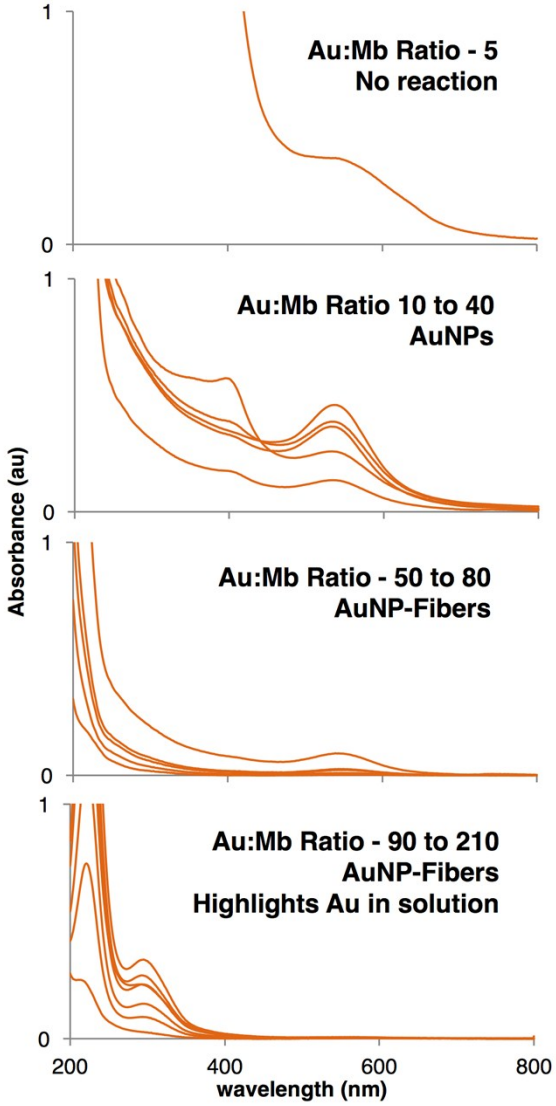

S21. UV-Vis spectra of pepsin biotemplating reactions

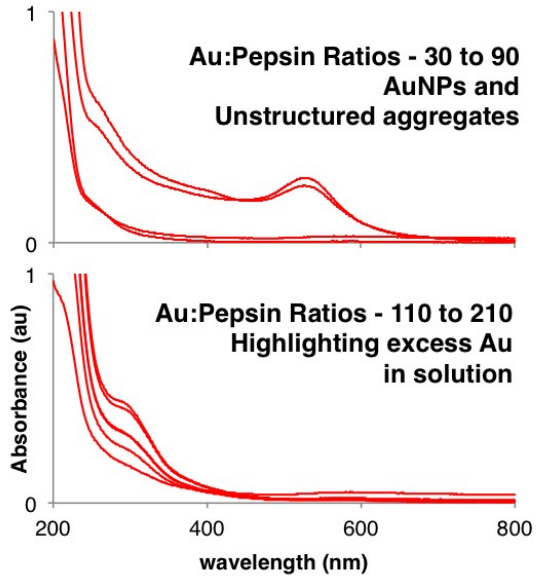

By plotting the absorbance value of the SPR feature (squares) along with the gold concentration as measured by AA (circles), we can determine the critical ratio, which describes the protein concentration where the biotemplating products change from AuNPs to AuNP fibers

S22. BSA-AuNP UV-Vis and AA data

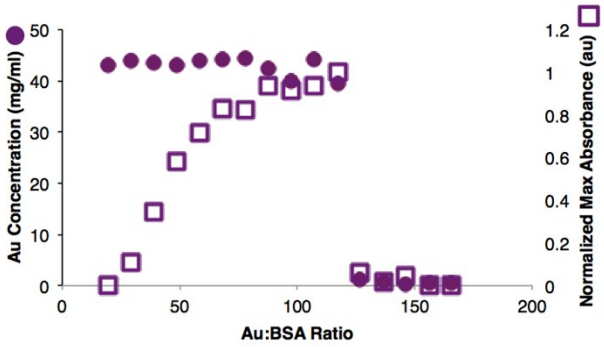

S23. Hemoglobin-AuNP UV-Vis and AA-data

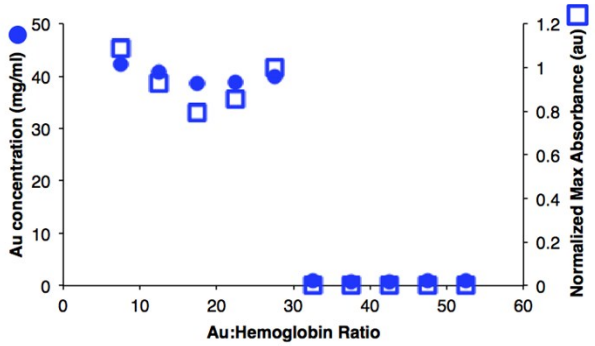

S24. Lysozyme-AuNP UV-Vis and AA-data

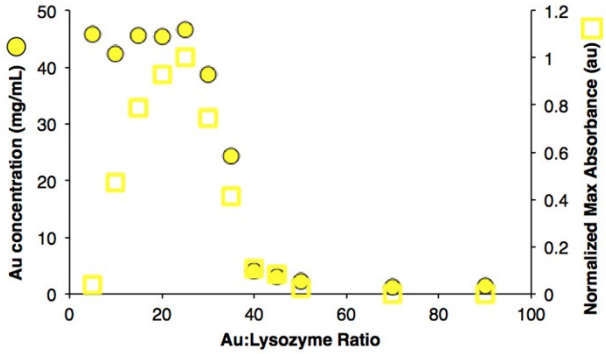

S25. Myoglobin-AuNP UV-Vis and AA-data

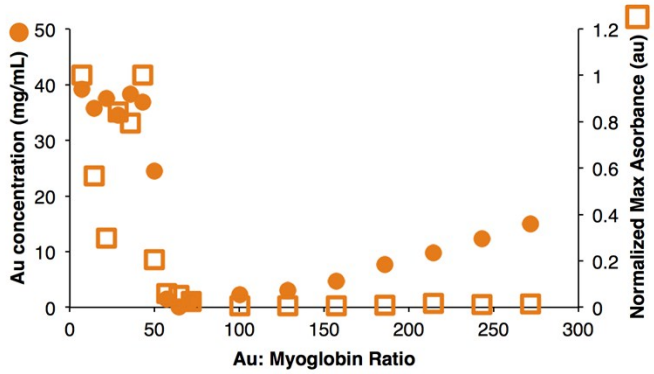

S26. Pepsin-AuNP UV-Vis and AA-data

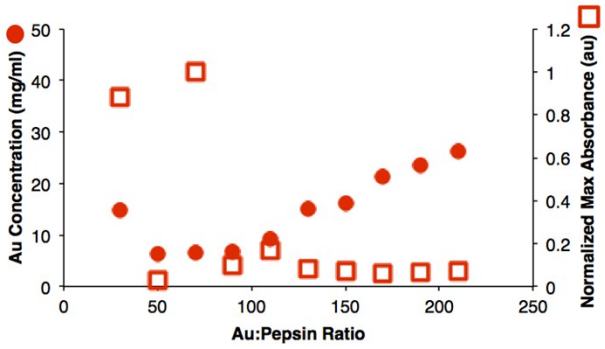

V. Gold nanoparticle formation kinetics

Nanoparticle formation kinetics were analyzed from spectra recorded with an Ocean Optics Jaz spectrometer. A capped cuvette, containing the reaction mixture, was placed in a temperature controlled cuvette holder (qpod 2e from Quantum Northwest). Individual spectra were recorded every 120 seconds (in most cases) until the nanoparticle formation reaction had nearly reached its end point. Reactions were monitored at 60, 70, 80, and 90 °C. The kinetics of nanoparticle formation was analyzed by subtracting the absorption minimum (just before the localized surface plasmon feature, LSP) from the absorption at the LSP maximum. These features are indicated in Figure S27. These ΔA values are then normalized to better highlight the reaction endpoints.

S27. Spectra from multiple times for the reaction of BSA with $HAuCl_4$. Figure highlights the data analysis used for evaluating the reaction kinetics.

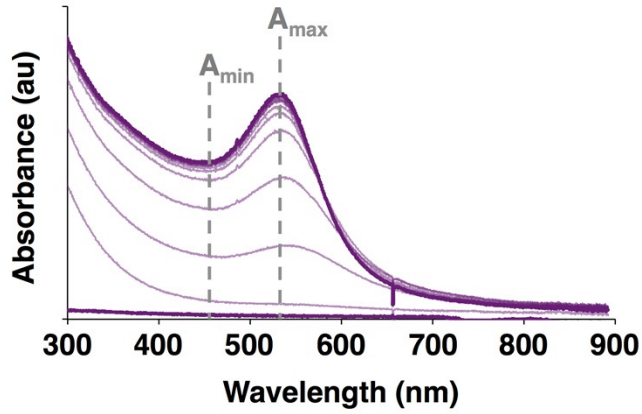

S28. Normalized(A_{max}-A_{min}) vs. time for BSA at 60, 70, 80, and 90 °C for Au:BSA ratios of 90 (purple), which produce homogenous BSA-AuNPs, and 150 (gray), which produce BSA-AuNP fibers.

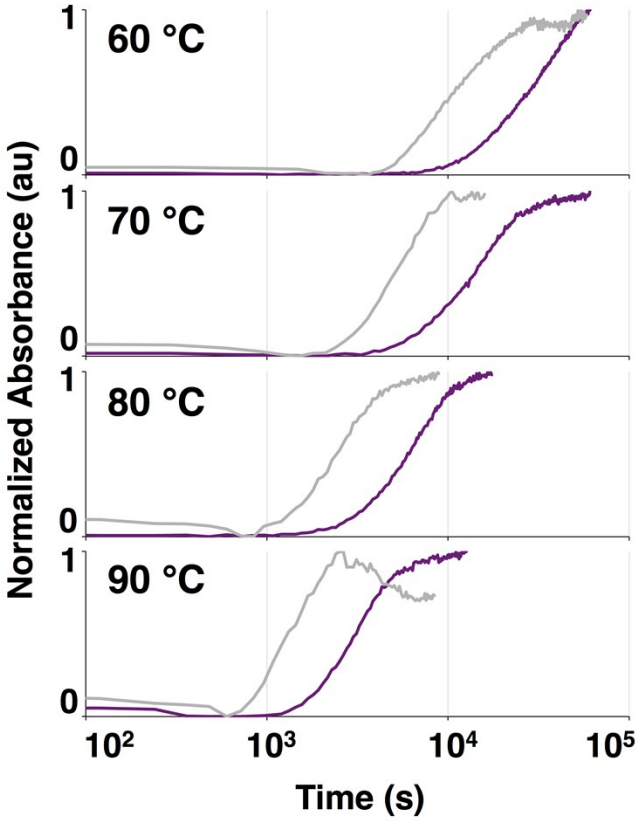

S29. Normalized(A_{max}-A_{min}) vs. time for catalase at 60, 70, 80, and 90 °C for Au:catalase ratios of 60 (dark blue), which produce homogenous catalase-AuNPs, and 110 (gray), which produce catalase-AuNP fibers.

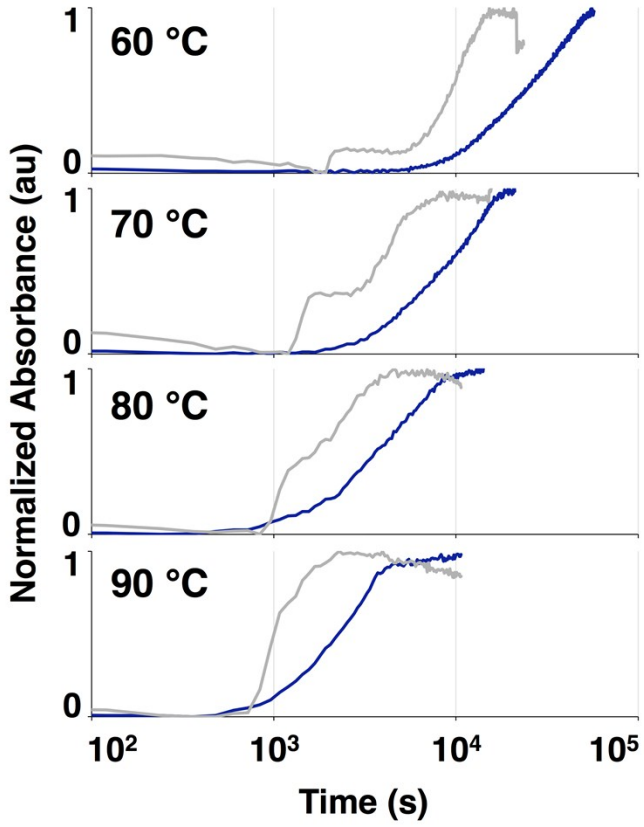

S30. Normalized(A_{max}-A_{min}) vs. time for hemoglobin at 60, 70, 80, and 90 °C for Au:hemoglobin ratios of 20 (blue), which produce homogenous hemoglobin-AuNPs, and 40 (gray), which produce hemoglobin-AuNP fibers.

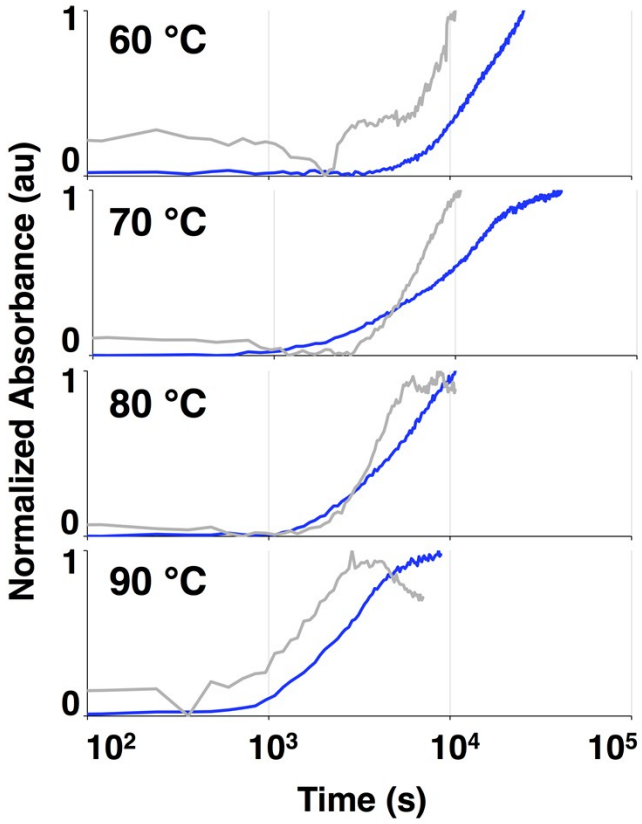

S31. Normalized(A_{max}-A_{min}) vs. time for lysozyme at 60, 70, 80, and 90 °C for Au:lysozyme ratios of 25 (blue), which produce homogenous lysozyme-AuNPs, and 55 (gray), which produce lysozyme-AuNP fibers.

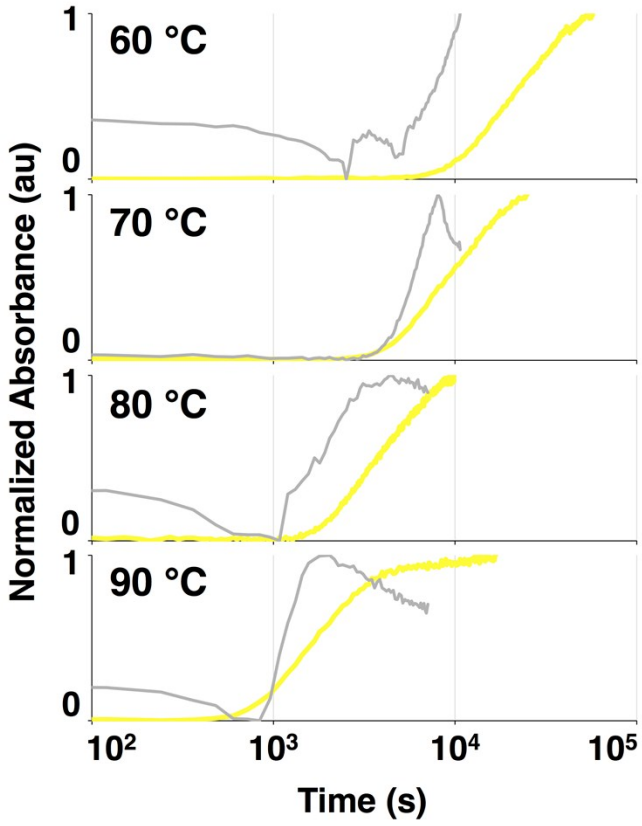

Table 1. Proteins, AuNP/AuNP fiber critical ratio values, and biotemplating relevant protein properties.

	BSA	Catalase	Hemoglobin	HRP	Invertase	Lysozyme	Myoglobin	Pepsin
Critical Ratio (moles Au:moles protein)	**125**	**80**	**30**	-	-	**35**	**35**	-
Critical Ratio (moles Au:10^3 g protein)	1.9	1.3	1.9	-	-	2.4	2.1	-
Molecular Weight (Da)	66,430	62,500	16,125	44,000	270,000	14,307	17,600	34,620
Number of Ligating Amino Acids[a]	153	103	24	43	77	20	35	52
Number of Reducing Amino Acids[a]	36	26	4	10	49	11	5	24
pI	5.3[2]	5.4[3]	6.8[4]	3-9[5]	4[6]	11.35[7]	7.3[8]	2.5[9]
% Structured[a]	76	56	82	47	52	74	57	71
Secondary Structure Unfolding Temperature (°C)	80[10]	56[11]	65[12]	82[13]	-	70[14]	80[15]	63[16]
Tertiary Structure Unfolding Temperature (°C)	68[17]	56[11]	50[18]	55[13]	65[19]	65[20]	75[21]	63[22]
Average Protein Hopp-Woods Hydrophobicity[b]	0.281	0.048	-0.081	-0.100	-0.154	-0.048	0.170	-0.282

[a]The numbers of ligating and reducing amino acids and the percentage of the protein that is structured were taken from data in UniProt.[23] (BSA - UniProt code: P02769, catalase - P00432, hemoglobin - P07020 and P01966, invertase - P10594, lysozyme - P00698, myoglobin - P68082, and pepsin - P00791). Structural data from HRP was gathered from a specific crystal structure.[24]

[b]The average Hopp-Woods[25] hydrophobicity measurement was performed using the ExPasy tools.[26]

VI. References

1. M. R. Hartings, N. Benjamin, F. Briere, M. Briscione, O. Choudary, T. L. Fisher, L. Flynn, E. Ghias, M. Harper, N. Khamis, C. Koenigsknecht, K. Lazor, S. Moss, E. Robbins, S. Schultz, S. Yaman, L. M. Haverhals, P. C. Trulove, H. C. De Long, A. E. Miller and D. M. Fox, *Sci. Technol. Adv. Mat.*, 2013, **14**.
2. J. F. Foster and L. J. Kaplan, *Biochemistry*, 1971, **10**, 630-636.
3. T. Samejima, M. Kamata and K. Shibata, *J. Biochem.*, 1962, **51**, 181-187.
4. H. Kon and M. W. Makinen, *Biochemistry*, 1971, **10**, 43-52.
5. L. M. Shannon, E. Kay and J. Y. Lew, *J. Biol. Chem.*, 1966, **241**, 2166-2172.
6. P. G. Righetti and T. Caravaggio, *J. Chromatog. A*, 1976, **127**, 1-28.
7. L. R. Wetter and H. F. Deutsch, *J. Biol. Chem.*, 1951, **192**, 237-242.
8. B. J. Radola, *BBA-Prot. Struct.*, 1973, **295**, 412-428.
9. D. Malamud and J. W. Drysdale, *Anal. Biochem.*, 1978, **86**, 620-647.
10. Y. Moriyama, E. Watanabe, K. Kobayashi, H. Harano, E. Inui and K. Takeda, *J. Phys. Chem. B*, 2008, **112**, 16585-16589.
11. J. Switala, J. O. O'Neil and P. C. Loewen, *Biochemistry*, 1999, **38**, 3895-3901.
12. A. Michnik, Z. Drzazga, A. Kluczewska and K. Michalik, *Biophys. Chem.*, 2005, **118**, 93-101.
13. K. Chattopadhyay and S. Mazumdar, *Biochemistry*, 1999, **39**, 263-270.
14. Y. J. Shiu, U. S. Jeng, Y. S. Huang, Y. H. Lai, H. F. Lu, C. T. Liang, I. J. Hso, C. H. Su, C. Su, I. Chao, A. C. Su and S. H. Lin, *Biophys. J.*, 2008, **94**, 4828-4836.
15. Y. Moriyama and K. Takeda, *J. Phys. Chem. B*, 2010, **114**, 2430-2434.
16. S. R. Tello-Solis and B. Romero-Garcia, *Int. J. Biol. Macromol.*, 2001, **28**, 129-133.
17. A. Michnik, K. Michalik, A. Kluczewska and Z. Drzazga, *J. Therm. Anal. Calorim.*, 2006, **84**, 113-117.
18. Y. B. Yan, Q. Wang, H. W. He and H. M. Zhou, *Biophys. J.*, 2004, **86**, 1682-1690.
19. D. Cavaille and D. Combes, *J. Biotechnol.*, 1995, **43**, 221-228.
20. F. Meersman, C. Atilgan, A. J. Miles, R. Bader, W. F. Shang, A. Matagne, B. A. Wallace and M. H. J. Koch, *Biophys. J.*, 2010, **99**, 2255-2263.
21. F. Meersman, L. Smeller and K. Heremans, *Biophys. J.*, 2002, **82**, 2635-2644.
22. V. M. Pavelkic, M. V. Beljanski, K. M. Antic, M. M. Babic, T. P. Brdaric and K. R. Gopcevic, *Russ. J. Phys. Chem. A*, 2011, **85**, 2245-2250.
23. M. Magrane and C. UniProt, *Database*, 2011.
24. G. I. Berglund, G. H. Carlsson, A. T. Smith, H. Szoke, A. Henriksen and J. Hajdu, *Nature*, 2002, **417**, 463-468.
25. T. P. Hopp and K. R. Woods, *Proc. Natl. Acad. Sci., USA*, 1981, **78**, 3824-3828.
26. E. Gasteiger, A. Gattiker, C. Hoogland, I. Ivanyi, R. D. Appel and A. Bairoch, *Nucleic Acids Res.*, 2003, **31**, 3784-3788.